

Modeling Steady Acoustic Fields Bounded in Cavities with Geometrical Imperfections

P. A. Giuliano Albo · R. M. Gavioso ·
G. Benedetto

Received: 15 February 2010 / Accepted: 19 June 2010 / Published online: 27 July 2010
© Springer Science+Business Media, LLC 2010

Abstract A mathematical method is derived within the framework of classical Lagrangian field theory, which is suitable for the determination of the eigenstates of acoustic resonators of nearly spherical shape. The method is based on the expansion of the Helmholtz differential operator and the boundary condition in a power series of a small geometrical perturbation parameter ϵ . The method extends to orders higher than ϵ^2 the calculation of the perturbed acoustic eigenvalues, which was previously limited by the use of variational formalism and the methods of Morse and Ingard. A specific example is worked out for radial modes of a prolate spheroid, with the frequency perturbation calculated to order ϵ^3 . A possible strategy to tackle the problem of calculating the acoustic eigenvalues for cavities presenting non-smooth geometrical imperfections is also described.

Keywords Acoustic eigenvalues · Quasi-spherical resonators · Shape perturbation theory

1 Introduction

A number of different experimental methods are currently being developed in a quest to pursue a determination of the Boltzmann constant k_B with an overall relative uncertainty below 1 ppm [1]. Among these, the determination of the speed of sound in a gas-filled spherical cavity by measuring its acoustic and microwave resonance frequencies, looks promising in reason of the results obtained so far [2–4]. To further increase the achievable accuracy, these experiments rely on the development

P. A. G. Albo (✉) · R. M. Gavioso · G. Benedetto
Istituto Nazionale di Ricerca Metrologica, Strada delle Cacce 91, 10135 Torino, Italy
e-mail: a.albo@inrim.it

of theoretical models which account for major perturbing effects, including the perturbation induced by the imperfect geometry of the resonator. This imperfection may be intentionally designed, as in the case of triaxial ellipsoidal cavities [5], to ease the precise determination of the mean frequency of degenerate microwave eigenfunctions. In addition, the limits of fabricating techniques, and those associated to the experimental procedures used to assemble the two hemispheres comprising the cavity, concur in making the final geometry of the resonator different from the initial design.

In geometrical perturbation models, it is common to assume that the shape of the assembled resonator is only slightly different from a sphere, the difference being described using a parameter ϵ , which is a small fraction of unity. Thus, the surface of the imperfect resonator and that of a perfect sphere coincide in the limit $\epsilon \rightarrow 0$. The historical development of the mathematical tools used to calculate geometrical corrections to the acoustic and microwave eigenvalues of quasi-spherical resonators, was initiated by Mehl's [6, 7] demonstration that the first non-vanishing corrections to the acoustic eigenvalues are of order ϵ^2 for arbitrary shape deformations which are volume-preserving. Recently, second-order geometrical corrections for the acoustic [8] and microwave [9] eigenvalues were derived for prolate and oblate spheroid and triaxial ellipsoids. Finally, the calculation of acoustic perturbed eigenvalues was extended to the more general case of a resonator whose shape is expressed by a series of spherical harmonics [10]. With these achievements in mind, we point out that the currently available theoretical framework may not be sufficiently complete to accomplish a speed-of-sound measurement achieving the accuracy goal stated above. Specifically, the availability of a perturbative method capable of extending the calculation of the geometrical corrections to higher order in ϵ , and suitable to deal with the case of non-smooth geometrical imperfections (like the step-like equatorial disjunction caused by the imperfect alignment of the two cavities comprising the resonator) would be most welcome. As a possible solution to these open problems, we describe an iterative operatorial method, whose peculiar features do not limit to a particular order the calculation of the geometrically perturbed acoustic eigenstates of a quasi-spherical cavity. As a practical application example, the method is used to work out analytically the third-order geometrical corrections to the radial modes of a prolate spheroid. By choosing $\epsilon = 1 \times 10^{-3}$, the relative difference between the eigenvalues, respectively, calculated at order ϵ^3 and ϵ^2 for the modes (0,2) to (0,8) is found to vary between 0.002 and -1.06 parts in 10^6 .

Finally, we discuss the perspectives of an analytical and a numerical approach in the application of the operatorial method to calculate the perturbations induced by non-smooth geometrical defects.

2 Basis of the Operatorial Method

The problem of determining the natural modes of an acoustic field, ψ , bounded in a cavity with a perfect spherical shape can be translated in the following system of two partial differential equations:

$$\left[\frac{\partial^2}{\partial r^2} + \frac{2}{r} \frac{\partial}{\partial r} + \frac{\partial^2}{r^2 \partial \theta^2} + \frac{\cos(\theta)}{r^2 \sin(\theta)} \frac{\partial}{\partial \theta} + \frac{\partial^2}{r^2 \sin^2(\theta) \partial \phi^2} + {}^0k^2 \right] \cdot \psi(r, \theta, \phi) = 0 \quad (S)$$
(1a)

$$\mathbf{n} \cdot \nabla \psi = 0 \quad (\partial S) \quad (1b)$$

where the shape of the cavity, S , is parametrized using spherical coordinates (r, θ, ϕ) . The differential operator appearing in the *Helmholtz equation* (1a), is usually written in a shorter form as $({}^0H + {}^0k^2) \cdot \psi = 0$. The *Neumann boundary conditions* in Eq. 1b fix the properties of the acoustic field on internal cavity wall ∂S ; particularly, they impose that the derivative calculated in the direction \mathbf{n} , normal to the surface of the cavity, must be null. The unknown variables of this system are the eigenvalues 0k and the eigenfunctions $\psi(r, \theta, \phi)$. From a physical point of view, the system (Eq. 1) imposes that the field ψ evolves according to the *minimum action principle* and that it does not lose energy exchanging momentum with the shell. This problem can be solved exactly for a perfect sphere, thanks to the property of the equation to admit a separable solution ${}^0\psi$.

When the cavity shape is not perfectly spherical, the corresponding equation is no longer separable and the solution cannot be found exactly, but only in terms of successive approximations. In the following, we consider the particular case of a resonant cavity of *quasi-spherical* shape. A surface M is a quasi-sphere (QS) when its parametrization M depends on a perturbation parameter ϵ and $M(\epsilon)$ becomes a perfect sphere in the limit $\epsilon \rightarrow 0$. By way of examples, two different kinds of parametrizations for $M(\epsilon)$ are reported:

$$M(\epsilon) = \begin{cases} x = r(1 - \epsilon) \sin(\theta) \cos(\phi) \\ y = r(1 - \epsilon) \sin(\theta) \sin(\phi) \\ z = r \cos(\theta) \end{cases} \quad (2a)$$

$$M(\epsilon) = \begin{cases} x = r[1 - \epsilon F(\theta, \phi)] \sin(\theta) \cos(\phi) \\ y = r[1 - \epsilon F(\theta, \phi)] \sin(\theta) \sin(\phi) \\ z = r[1 - \epsilon F(\theta, \phi)] \cos(\theta). \end{cases} \quad (2b)$$

The system of Eq. 2a represents a prolate spheroid, while Eq. 2b is a more general parametrization describing shapes non-necessarily symmetric.

The Helmholtz equation associated to the manifold $M(\epsilon)$ can be built using the *Lagrangian density* $\mathcal{L}(\psi, \nabla \psi) = {}^\tau(\nabla \psi) \cdot \bar{g} \cdot \nabla \psi$, where the metric tensor \bar{g} is obtained from the Jacobian matrix $J(\epsilon)$, associated to $M(\epsilon)$, as

$$\bar{g}(\epsilon) = ({}^\tau J \cdot J)^{-1}. \quad (3)$$

Using the *Euler–Lagrange* equation applied to \mathcal{L} , it is possible to obtain the operator $H(\epsilon)$ representing the Helmholtz equation associated to $M(\epsilon)$,

$$[H(\epsilon) + k^2(\epsilon)] \cdot \psi = {}^\tau \nabla \cdot [\sqrt{\bar{g}} \bar{g}(\epsilon) \cdot \nabla \psi] + k^2(\epsilon) \psi = 0, \quad (4)$$

where $\sqrt{g} = \sqrt{\det(\bar{g})^{-1}}$ and the dependence of the operator H , and the eigenvalue k , from the perturbation parameter ϵ are evidenced. A similar approach can be used to rewrite the boundary conditions, with reference to the manifold $M(\epsilon)$, leading to

$$\mathbf{n}(\epsilon) \cdot \nabla \psi = 0. \quad (5)$$

The solution of Eqs. 4 and 5 can be obtained in an approximated form by assuming that the exact solution ψ can be expanded in a Taylor series in terms of ϵ around the point $\epsilon = 0$ as

$$\psi = {}^0\psi + {}^1\psi \epsilon + {}^2\psi \epsilon^2 + {}^3\psi \epsilon^3 + \dots, \quad (6)$$

where the functions ${}^n\psi$ are unknown and do not depend on ϵ . Analogous expressions can be obtained for the operator $H(\epsilon) = {}^0H + {}^1H\epsilon + {}^2H\epsilon^2 + {}^3H\epsilon^3 + O(\epsilon^4)$, the eigenvalue $k^2 = {}^0k^2 + {}^1k^2\epsilon + {}^2k^2\epsilon^2 + {}^3k^2\epsilon^3 + O(\epsilon^4)$, and for the normal vector $\mathbf{n}(\epsilon) = {}^0\mathbf{n} + {}^1\mathbf{n}\epsilon + {}^2\mathbf{n}\epsilon^2 + {}^3\mathbf{n}\epsilon^3 + O(\epsilon^4)$. Substituting Eq. 6 into Eqs. 4 and 5, considering the expanded expressions for the other terms appearing in these equations, and collecting terms at the same order ϵ , the problem of Eqs. 4 and 5 can be reformulated as

$$\begin{cases} ({}^0H + {}^0k) \cdot {}^0\psi = 0 \\ {}^0\mathbf{n} \cdot \nabla {}^0\psi = 0 \end{cases} \quad (7)$$

$$\begin{cases} ({}^1H + {}^1k) \cdot {}^0\psi + ({}^0H + {}^0k) \cdot {}^1\psi = 0 \\ {}^1\mathbf{n} \cdot \nabla {}^0\psi + {}^0\mathbf{n} \cdot \nabla {}^1\psi = 0 \end{cases} \quad (8)$$

$$\begin{cases} ({}^2H + {}^2k) \cdot {}^0\psi + ({}^1H + {}^1k) \cdot {}^1\psi + ({}^0H + {}^0k) \cdot {}^2\psi = 0 \\ {}^2\mathbf{n} \cdot \nabla {}^0\psi + {}^1\mathbf{n} \cdot \nabla {}^1\psi + {}^0\mathbf{n} \cdot \nabla {}^2\psi = 0 \end{cases} \quad (9)$$

$$\begin{cases} ({}^3H + {}^3k) \cdot {}^0\psi + ({}^2H + {}^2k) \cdot {}^1\psi + ({}^1H + {}^1k) \cdot {}^2\psi \\ + ({}^0H + {}^0k) \cdot {}^3\psi = 0 \\ {}^3\mathbf{n} \cdot \nabla {}^0\psi + {}^2\mathbf{n} \cdot \nabla {}^1\psi + {}^1\mathbf{n} \cdot \nabla {}^2\psi + {}^0\mathbf{n} \cdot \nabla {}^3\psi = 0 \end{cases} \quad (10)$$

where just the unperturbed (Eq. 7), the first (Eq. 8), the second (Eq. 9), and the third-order (Eq. 10) problems are explicitly shown, although the procedure can be extended to higher orders of approximation.

For quasi-spheres, the unperturbed problem of Eq. 7 is coincident with Eq. 1; thus, the function ${}^0\psi$ and the eigenvalue 0k must be considered known terms in Eqs. 8 to 10 together with nH and ${}^n\mathbf{n}$ for which an explicit expression has been built from the parametrization (Eq. 2).

It is worth noticing that, at any order, the solution for the function ${}^n\psi$ can be obtained when the solution ${}^{(n-1)}\psi$ is known and when the inverse of the operator $({}^0H + {}^0k^2)$, namely, $R = ({}^0H + {}^0k^2)^{-1}$ is built. Usually, the resolvent operator R is expressed using opportune Green functions, depending on the particular choice of the

unperturbed function ${}^0\psi$. For example, applying R to the first-order approximation problem, the following expression is obtained:

$${}^1\psi_p = -R[({}^1H + {}^1k) \cdot {}^0\psi], \quad (11)$$

where the solution ${}^1\psi_p$ is just a particular solution that usually does not satisfy the boundary conditions (Eq. 8). The complete solution can be obtained adding to Eq. 11 an opportune solution of the unperturbed operator, chosen to verify the boundary conditions. The first-order eigenvalue ${}^1k^2$ can be calculated as

$${}^1k^2 = \frac{\int \sqrt{{}^0g} {}^0\psi {}^1H \cdot {}^0\psi dM}{\int \sqrt{{}^0g} {}^0\psi {}^0\psi dM}. \quad (12)$$

This expression can be obtained considering that the operator $({}^0H + {}^0k^2)$ is self-adjoint and integrating over the volume the first-order problem in Eq. 8 multiplied by ${}^0\psi$. The second-order approximations are calculated following the same procedure applied to the first-order problem with ${}^1\psi$ and 1k being now known. The resolution method can be iterated to obtain higher-order approximations.

3 Prolate Spheroid: Third-Order Corrections

As an example of application of the operatorial method, in the following, we detail the calculation of radial modes of a prolate spheroid.

A prolate spheroid M is a quasi-sphere parametrized by Eq. 2a. Using Eq. 5 the exact Helmholtz equation can be obtained and the perturbation operators are

$$\left\{ \begin{array}{l} {}^0H = \partial_{rr} + \frac{2}{r}\partial_r + \frac{1}{r^2}\partial_{\theta\theta} + \frac{\cos(\theta)}{r^2\sin(\theta)}\partial_\theta + \frac{1}{r^2\sin^2(\theta)}\partial_{\varphi\varphi} \\ {}^1H = 2\sin^2(\theta)\partial_{rr} - \frac{3+\cos(2\theta)}{r}\partial_r + \frac{2\cos^2(\theta)}{r^2}\partial_{\theta\theta} + \frac{4\cos(\theta)\sin(\theta)}{r}\partial_{r\theta} + \\ \quad + \frac{2\cos(2\theta)\cos(\theta)}{r^2\sin(\theta)}\partial_\theta + \frac{2}{r^2\sin^2(\theta)}\partial_{\varphi\varphi} \\ {}^2H = \frac{3}{2}{}^1H \\ {}^3H = \frac{4}{3}{}^2H = 2{}^1H. \end{array} \right. \quad (13)$$

The parametrization (Eq. 2a) does not allow one to obtain a separable Helmholtz equation; however, for the operatorial method this is not a necessary requirement.

The first-order corrections terms ${}^1k^2 = 4/3 {}^0k^2$ can be obtained using Eq. 12. The perturbed eigenvalue $k^2 = {}^0k^2 + {}^1k^2 \epsilon + O(\epsilon^2)$ is coincident with that of a perfect sphere having the same volume of the prolate spheroid as widely discussed in [6] and [7].

The known term ${}^1\eta = ({}^1H + {}^1k^2) \cdot {}^0\psi$ can be decomposed as ${}^1\eta = \alpha_{00}(r)Y_{00} + \alpha_{20}(r)Y_{20}$ where Y_{lm} are spherical harmonic functions, so that the first-order correction ${}^1\psi$ can be obtained as

$$\begin{aligned} & {}^1\psi(\rho, \theta, \phi) \\ &= -Y_{00}(\theta, \phi) \left[\int_0^\rho r^2 \frac{y_0({}^0k\rho)j_0({}^0kr)}{wp_l} \alpha_{00} dr + \int_\rho^1 r^2 \frac{j_0({}^0k\rho)y_0({}^0kr)}{wp_l} \alpha_{00} dr \right] + \\ &\quad - Y_{20}(\theta, \phi) \left[\int_0^\rho r^2 \frac{y_2({}^0k\rho)j_2({}^0kr)}{wp_l} \alpha_{20} dr + \int_\rho^1 r^2 \frac{j_2({}^0k\rho)y_2({}^0kr)}{wp_l} \alpha_{20} dr \right] + \\ &\quad + c_{20} j_2({}^0kr) Y_{20}(\theta, \phi). \end{aligned} \quad (14)$$

In Eq. 14, wp_l is the Wronskian of the Bessel functions $j_l(z)$ and $y_l(z)$, of the first- and the second-kind, respectively, multiplied by r^2 , and c_{20} is a constant which must satisfy the first-order boundary conditions.

Once the function ${}^1\psi$ is determined, the second-order correction ${}^2k^2$ can be calculated from the following equation, where the only unknown is ${}^2k^2$:

$$\begin{aligned} \int \sqrt{{}^n g} {}^0\psi ({}^2H + {}^2k^2) \cdot {}^0\psi dM &= - \int \sqrt{{}^0 g} {}^1\psi ({}^1H + {}^1k^2) \cdot {}^0\psi dM + \\ &\quad - \int \sqrt{{}^1 g} {}^0\psi ({}^1H + {}^1k^2) \cdot {}^0\psi dM \end{aligned} \quad (15)$$

and the term $\sqrt{{}^n g}$ is the n -coefficients of the Taylor expansion of $\sqrt{g(\epsilon)}$. Remarkably, the results, which are listed in Table 1, are found in agreement with those reported in

Table 1 Prolate spheroid: second- and third-order relative corrections to the squared eigenvalues for the radial modes (0,2)–(0,8)

Radial mode	Second-order theory		Third-order theory		
	$10^6(k^2 - k_{eq}^2)/{}^0k^2$	$10^6O({}^0k^2 \epsilon^3)$	$10^6(k^2 - k_{eq}^2)/{}^0k^2$	$10^6O({}^0k^2 \epsilon^4)$	$10^6{}^3k^2 / {}^0k^2 \epsilon^3$
(0, 2)	1.19648762	0.0202	1.19808744	0.00002	0.0016
(0, 3)	3.53656391	0.0597	3.53242567	0.00006	-0.004
(0, 4)	7.04591817	0.1189	7.01118073	0.0001	-0.035
(0, 5)	11.7249073	0.1979	11.6083224	0.0002	-0.117
(0, 6)	17.5735948	0.2966	17.2887303	0.0003	-0.285
(0, 7)	24.5919991	0.4150	24.0084427	0.0004	-0.584
(0, 8)	32.7801272	0.5532	31.7146905	0.0006	-1.065

The corrections are relative to the squared eigenvalues of a perfect sphere of equivalent volume, and are calculated for $\epsilon = 1 \times 10^{-3}$. The estimated residual contributions from the higher-order terms are listed as $O({}^0k^2 \epsilon^3)$ for the calculation truncated at the second-order and $O({}^0k^2 \epsilon^4)$ for calculation truncated at the third order. The relative difference between the eigenvalues calculated at second- and third-order is listed in the rightmost column

[6] and [7] for the second-order corrections to the eigenvalues of the radial modes. However, a further improvement introduced by the operatorial method is its possibility to be extended to the determination to higher order.

The third-order corrections ${}^3k^2$ can be determined once that the function ${}^2\psi$ is obtained from the solution of Eq. 9, which can be solved using the same method applied to determine ${}^1\psi$. The only difference is that the term $({}^1H + {}^1k^2).{}^1\psi$ generates further Y_{20} and Y_{40} components, so that the resolvent has two more integrals and two further functions: $b_{20}j_2({}^0kr)Y_{20}(\theta, \phi)$ and $b_{40}j_4({}^0kr)Y_{40}(\theta, \phi)$. Again the integration constants b_{20} and b_{40} must be adjusted to satisfy boundary conditions and ${}^3k^2$ is calculated integrating over the volume M the following expression: $\sqrt{^2g}{}^0\psi({}^1H + {}^1k^2).{}^0\psi + \sqrt{^1g}{}^1\psi({}^1H + {}^1k^2).{}^0\psi + \sqrt{^1g}{}^0\psi({}^2H + {}^2k^2).{}^0\psi + \sqrt{^0g}{}^2\psi({}^1H + {}^1k^2).{}^0\psi + \sqrt{^0g}{}^1\psi({}^2H + {}^2k^2).{}^0\psi + \sqrt{^0g}{}^0\psi({}^3H + {}^3k^2).{}^0\psi$.

In Table 1 the relative differences between the perturbed squared eigenvalues k^2 calculated at the second- and the third-order in ϵ , with $\epsilon = 1 \times 10^{-3}$ and the unperturbed eigenvalues of the perfect sphere of equivalent volume k_{eq}^2 , are reported. The correction increases with the mode number, and amounts to about 1 ppm for mode (0,7). It is worth noticing that the residual $O({}^0k^2 \epsilon^3)$ and the estimated correction ${}^3k^2 / {}^0k^2 \epsilon^3$ are commensurate, supporting the validity of the results.

4 Non-smooth Geometries

In the following, we describe the perspective and the difficulties encountered in an attempt to apply the operatorial method to the case of cavities characterized by non-smooth boundaries.

4.1 Perspective of an Analytical Approach

The geometrical parametrization of a quasi-sphere, whose shape presents non-smooth defects, may be conveniently expressed using a *morphing* (the term is borrowed from image processing algorithms) parameter a . For example, the parametrization $M(\epsilon)$ of a cavity composed by two hemispheres having different radii may be expressed as

$$M(\epsilon, a) = \begin{cases} x = r[1 - \epsilon F(\theta, a)] \sin(\theta) \cos(\phi) \\ y = r[1 - \epsilon F(\theta, a)] \sin(\theta) \sin(\phi) \\ z = r[1 - \epsilon F(\theta, a)] \cos(\theta), \end{cases} \quad (16)$$

where $F(\theta, a) = 1/\pi \arctan(\cos(\theta)/a)$. A second example, using the same definition of $F(\theta, a)$, expresses the parametrization for a misaligned resonator,

$$M(\epsilon, a) = \begin{cases} x = r[\sin(\theta) \cos(\phi) + \epsilon F(\theta, a)] \\ y = r \sin(\theta) \sin(\phi) \\ z = r \cos(\theta) \end{cases} \quad (17)$$

Figure 1 illustrates how the initially smooth surface of a perfect sphere is transformed into the discontinuous boundaries of the examples chosen above, in the limit

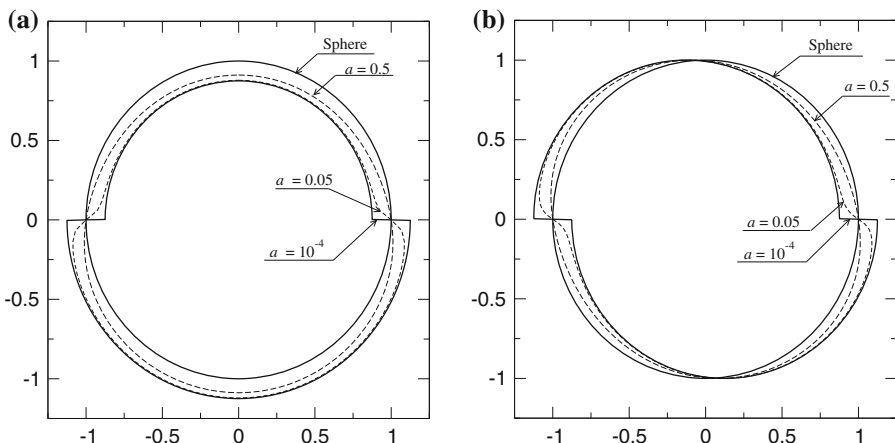


Fig. 1 Morphing of hemispheres (a) with different radii and (b) of misaligned hemispheres

$a \rightarrow 0$. Thus, in principle the operatorial method may be applied starting from the parametrization in Eqs. 16 and 17, by maintaining the parameter a undetermined. If the method succeeds in the determination of the perturbed eigenvalue, this will be a function $k(a)$ of the morphing parameter. Incidentally, we remark that parametrizations in Eqs. 16 and 17 may also be suitable to represent other geometrical imperfections which are typically present in acoustic thermometers like ducts, and annular slits.

Although the function $F(\theta, a)$ would be different for each particular case, the first-order correction to the unperturbed eigenfunction of radial modes can always be calculated as ${}^1\psi_p = {}^0k r j_1({}^0k r)F(\theta, a)$, where $j_1({}^0k r)$ is the spherical Bessel function of order 1.

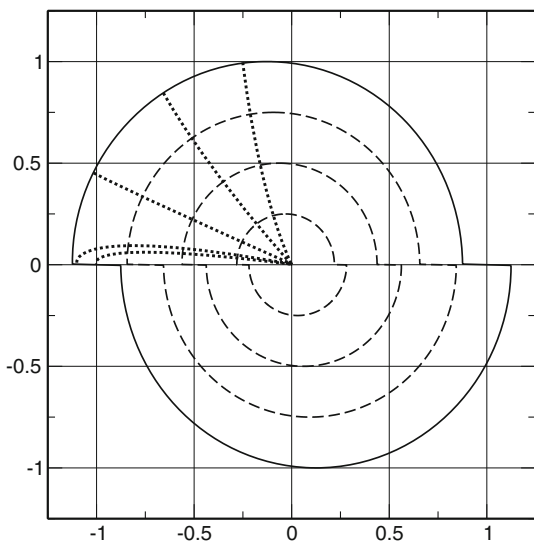
To be applicable, the analytical procedure just described needs further development, which is the subject of the current investigation. One difficulty is related to the suitable definition of boundary conditions on the discontinuous cavity surface which may not be represented as the sum of a finite number of unperturbed eigenfunctions which satisfy Eq. 8.

4.2 Numerical Approach

A numerical approach to the solution of the Helmholtz equation in perturbed geometries has already been investigated, and partially proved its effectiveness. Particularly, numerical methods based on finite-element (FEM) decomposition of the cavity shape are indicated to validate and check more accurate analytical results [8, 9].

We explored the possibility to adapt the peculiar features of the operatorial method to a numerical determination of the perturbed eigenvalues. We remark that such a numerical approach is strictly needed only for the determination of the second-order corrections ${}^2k^2$ because the unperturbed eigenvalues and the first-order corrections can always be obtained analytically.

Fig. 2 Examples of integration paths (dotted lines). The boundaries, shown using solid lines, should be scaled to represent the real dimension of the resonator



We make the trivial assumption that a solution which satisfies Eq. 4 over the entire volume of the cavity is also a solution of the same equation when limited on a spatial subset of the volume. Particularly, we chose to solve the Helmholtz equation on curves, in three-dimensional spaces, because the speed of convergence of the algorithm is very fast and stable.

To be effective, the numerical approach requires an opportune choice of the integration curves. As a matter of fact, if the chosen integration paths intercept the surface of the resonator with a direction normal to the tangent plane at the interception point, it is possible to transform the boundary conditions (Eq. 5) into initial conditions of the integration procedure. The choice of γ within a wide class of curves can be further restricted by observing that the parametrizations of Eqs. 16 and 17 share the common property of including the origin of the coordinate system allowing consideration of the parameter r as a simple scale factor. Figure 2 shows how the integration paths may start from the origin and remain always normal to each scaled intermediate surface. Under this condition, the eigenvalues can be simply determined using the *shooting method* [11], checking if the derivative of the field, calculated along the curve and evaluated on the surface is null, as the Neumann boundary conditions require.

The expression for the Helmholtz equation when restricted to an arbitrary curve could be obtained as a restriction of Eq. 5; however, a more intuitive method is suggested, which withdraws the scheme of the fluid dynamics when developed under the Lagrangian point of view or, in other words, following the motion of a particle moving in the flux of the fluid. Even if, in this representation, the integration line does no longer correspond to the direction of the motion of the acoustic wave, the similitude is useful to understand the origin of the conservation law.

Supposing that $\psi(r, \theta, \phi)$ is an eigenfunction of a steady acoustic field in the cavity, it is possible to show that Eq. 4 can be obtained applying the principle of minimum

action to the Lagrangian density $\mathcal{L} = \sqrt{\bar{g}}(\nabla\psi).\bar{g}.\nabla\psi$. The operator ∇ expresses the variation of the function ψ in the different directions; however, it is possible to limit this operator to a particular direction \mathbf{n} , considering the directional derivative $\mathbf{n}\cdot\nabla\psi$. In this new frame, the Lagrangian density $\mathcal{L} = \sqrt{\bar{g}}(\mathbf{n}\cdot\nabla\psi)^2$ and the corresponding Euler–Lagrange equation becomes

$$\frac{d^2\psi(s)}{ds^2} + (\nabla\cdot\mathbf{n})\frac{d\psi(s)}{ds} + k^2\psi(s) = 0 \quad (18)$$

where

$$\nabla\cdot\mathbf{n} = \sum_{i=1}^3 \left(\frac{\partial \mathbf{n}_i}{\partial q_i} + \sum_{k=1}^3 \Gamma_{k i}^k \mathbf{n}_i \right). \quad (19)$$

In Eq. 19, Γ is the Christoffel symbol determined by the metric \bar{g} , $q_i = (r, \theta, \phi)$ and s is the variable used to parametrize the integration path $\gamma(s)$. For example, in perfect spherical geometry $\nabla\cdot\mathbf{n} = 2/r$ and the corresponding equivalent of Eq. 18 is the Bessel equation which describes the propagation of radial modes when $s = r$.

More in general, the term $\nabla\cdot\mathbf{n}$ is a function of the coordinates (r, θ, ϕ) . Thus, to make the dependence of the coordinates from the parameter s explicit, the analytical expression of the integration path $\gamma(s) = \gamma(r(s), \theta(s), \phi(s))$ is needed. Given the arbitrariness of the integration curve, it is possible to substitute γ with its local first-order approximation:

$$\gamma(s + \Delta s) = \gamma(s) + \frac{d\gamma(s)}{ds} \Delta s + O(\Delta s^2) \quad (20)$$

preserving the accuracy of the solution. In Eq. 20, the term $d\gamma(s)/ds$ is the tangent vector to $\gamma(s)$ and, because of the shape of the chosen integration path, it coincides with \mathbf{n} . The integration path can be iteratively determined with the following procedure: first, a starting point $\gamma(s_0)$ is chosen; second, the vector \mathbf{n} is calculated at the same; and finally, a new point is determined along the integration path, in the direction of \mathbf{n} , at the distance specified by a step Δs .

The numerical solution of Eq. 18 can be obtained by its local representation in terms of Taylor coefficients $\psi(s_0)$, $d\psi(s_0)/ds$, and $d^2\psi(s_0)/ds^2$:

$$\psi(s_0 + \Delta s) = \psi(s_0) + \frac{d\psi(s_0)}{ds} \Delta s + \frac{1}{2} \frac{d^2\psi(s_0)}{ds^2} \Delta s^2 + O(\Delta s^3). \quad (21)$$

The first two coefficients can be fixed, as for any ordinary second-order differential equation, giving suitable initial conditions. For the case of a radial acoustic mode in quasi-spherical resonators, a possible choice is $s_0 = r = 0$, $\psi(0) = \text{const.}$, and $d\psi(0)/ds = 0$. Then the value of the coefficient $d^2\psi(s_0)/ds^2$ can be obtained from Eq. 18, with $k^2 = {}^0k^2 + {}^1k^2\epsilon$. The tangent vector to the integration path \mathbf{n} can be chosen arbitrarily when its expression is not defined in $r = 0$. The integration procedure can be iterated considering the point at $s_0 + \Delta s$ as the new starting point. Once

that the integration procedure is completed by reaching a point $\gamma(s_{\text{end}})$ on the cavity surface, the eigenvalue ${}^0k^2 + {}^1k^2 \epsilon$ determined with this procedure may be tested to check whether it represents an acceptable solution to the problem in Eq. 4, by verifying that $d\psi(s_{\text{end}})/ds = 0$. If this condition is not verified, a different eigenvalue may be determined and tested by using the *secant method* [12]. To be considered a satisfactory solution to the problem (Eq. 4), the determined eigenvalue must be a solution of Eq. 18 for any initial direction \mathbf{n} , arbitrary chosen.

5 Conclusions

The target of achieving an acoustic determination of the Boltzmann constant with a relative uncertainty below one part in 10^6 seemingly requires further development of the mathematical methods used to predict the perturbing effects induced by the geometrical imperfections of the cavity shape. The method and the examples presented in this work partially address this need, evidencing a sensible difference between the second- and third-order corrections to the acoustic eigenvalues of a prolate spheroid. Albeit the proposed method is not in principle limited with regard to the attainable order of approximation of the solutions or to a specific class of solvable geometries, the practical difficulties involved in the determination of appropriate resolving operators are relevant, currently limiting its applicability. A numerical approach to the application of the method may represent a valid simplification to these difficulties, and is the subject of the current investigation.

References

1. B. Fellmuth, C. Gaiser, J. Fischer, Meas. Sci. Technol. **17**, R145 (2006)
2. L. Pitre, C. Guianvarc'h, F. Sparasci, A. Guillou, D. Truong, Y. Hermier, M.E. Himbert, C.R. Phys. **10**, 835 (2009)
3. G. Sutton, R. Underwood, L. Pitre, M. De Podesta, S. Valkiers, Int. J. Thermophys. doi:[10.1007/s10765-010-0722-z](https://doi.org/10.1007/s10765-010-0722-z)
4. R.M. Gavioso, G. Benedetto, P.A. Giuliano Albo, D. Madonna Ripa, A. Merlone, C. Guianvarc'h, F. Moro, R. Cuccaro, Metrologia **47**, 387–409 (2010)
5. J.B. Mehl, M.R. Moldover, L. Pitre, Metrologia **31**, 295 (2004)
6. J.B. Mehl, J. Acoust. Soc. Am. **71**, 1109 (1982)
7. J.B. Mehl, J. Acoust. Soc. Am. **79**, 278 (1986)
8. J.B. Mehl, J. Res. Natl. Inst. Stand. Technol. **112**, 163 (2007)
9. J.B. Mehl, Metrologia **46**, 544 (2009)
10. J.B. Mehl, Int. J. Thermophys. doi:[10.1007/s10765-010-0731-y](https://doi.org/10.1007/s10765-010-0731-y)
11. W.H. Press, S.A. Teukolsky, W.T. Vetterling, B.P. Flannery, *Numerical Recipes in FORTRAN*, 2nd edn. (Cambridge University Press, London, 1992), p. 749
12. W.H. Press, S.A. Teukolsky, W.T. Vetterling, B.P. Flannery, *Numerical Recipes in FORTRAN*, 2nd edn. (Cambridge University Press, London, 1992), p. 347